PLANNING AND CONTROL OF PLANAR UNDERACTUATED MARINE VEHICLES SUBJECT TO LINEAR AND QUADRATIC DRAG

Filoktimon Repoulias, and Evangelos Papadopoulos
Department of Mechanical Engineering, National Technical University of Athens
15780 Athens, Greece
{firepoul, egpapado}@central.ntua.gr

ABSTRACT
This paper tackles the combined problem of trajectory planning and tracking control of planar underactuated marine vehicles with different dynamic models. A reference feasible trajectory for the position and orientation is planned so as to be consistent with each of the three dynamic models. Using these reference values the dynamics of the vehicles is transformed to the error one. Partial state-feedback linearization, backstepping and non-linear damping techniques are utilized to stabilize the above system and force the tracking error to a set of zero that can be made arbitrarily small. Simulation results are presented and discussed.

KEY WORDS
Underactuated vehicles, tracking, plane path

1. Introduction

Over the past two decades, there has been a considerable amount of research concerning the operation of autonomous vehicles because they can take man's place in hazardous environments: wheeled robots defuse mines, unmanned air vehicles take photographs of a battlefield, space robotic vehicles assist astronauts in repairing satellites. Autonomous marine vehicles (MV), such as hovercrafts, surface and underwater vehicles are playing a crucial role in the exploitation of oceanic resources.

Besides their numerous practical applications, these vehicles present a challenging control problem in the presence of nonholonomic constraints, or in case they are underactuated. Wheeled robots are subject to nonholonomic velocity constraints [3], whereas the nonholonomic behavior of space vehicles is due to the nonintegrability of the angular momentum conservation, [4]. Vehicles that have fewer actuators than degrees of freedom (DOF) are classified as underactuated and may either be air [5], or marine [1], [2]. Such control configuration imposes nonintegrable acceleration constraints that seriously affect their dynamic behavior.

This paper deals with the trajectory tracking control design for underactuated MV, i.e., surface vessels (SV), autonomous underwater vehicles (AUV) and hovercrafts (HC), in plane motion, Fig. 1. Although the operating environment of the latter is the air, it presents a similar dynamic model to that of an SV, [10].

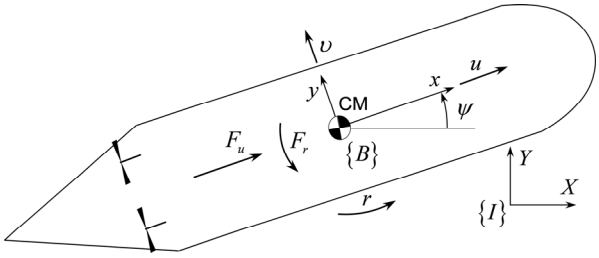

Fig. 1. Underactuated MV and motion variables.

MVs kinematic and dynamic models are highly nonlinear and coupled [2], making control design a hard task. Underactuation rules out the use of established control designs e.g. full state-feedback linearization [6], and the complex hydrodynamics (aerodynamics for HC) excludes designs based only on the kinematic model.

The stabilization problem -regulation to a point with a desired orientation- for underactuated MVs has been studied, e.g., in [7], and [8] which show that continuous time-invariant feedback control laws cannot asymptotically stabilize such vehicles.

Trajectory tracking deals with the design of control laws that force the vehicle to reach and track a time parameterized inertial trajectory, [10]. Tracking controller designs for underactuated MVs, currently in use, follow classical approaches such as local linearization and decoupling of the multivariable model to steer as many DOF as the available control inputs. Other solutions include the linearization of the vehicle's error dynamics about trimming trajectories which leads to time invariant linear systems followed by such techniques as gain scheduling, [5]. These solutions are limited in a small neighborhood around the operating points. Stability and performance also suffer when the MV executes manoeuvres that emphasize its complex hydrodynamics.

Theoretical and experimental results on trajectory tracking for underactuated MVs show that nonlinear Lyapunov-based techniques can overcome most of the limitations mentioned above. In [11], experimental tracking results for a model ship using Lyapunov-based controllers are presented. In [12], two tracking solutions

for an SV were proposed, based on Lyapunov's direct method and passivity approach. However, in those works, the yaw velocity was required to be nonzero. Under this restriction straight lines cannot be tracked. In [14], the error dynamics is transformed into a skew-symmetric form and practical convergence is achieved. In [10], the controller, exponentially forces the position error to a small neighbourhood of zero for MVs moving in two or three dimensions. However, the attitude is uncontrolled, which may lead to undesirable backward tracking. In [15], a trajectory planning and control method was presented for an AUV with linear drag in horizontal motion.

In this paper, we design a trajectory planning and tracking control law for three underactuated MVs with different dynamic models: an HC, an SV and an AUV with quadratic drag. The motion is considered to be planar. Results are excellent for the HC and the SV, since the tracking errors converge to a set of zero that can be made arbitrarily small. The error dynamics for the AUV are stable and the tracking errors oscillate in a bounded set close to zero but they cannot be eliminated completely.

2. Vehicle System Models

In this section, the kinematic and dynamic equations of an MV in horizontal motion are described. Using an inertial reference frame $\{I\}$ and a body-fixed frame $\{B\}$ with origin at the vehicle center of mass (CM) see Fig. 1, the kinematic equations of motion of the CM for an MV on the horizontal $X-Y$ plane are [2]:

$$\dot{x}=u\cos\psi-\upsilon\sin\psi \tag{1a}$$

$$\dot{y}=u\sin\psi+\upsilon\cos\psi \tag{1b}$$

$$\dot{\psi}=r \tag{1c}$$

where x and y represent the inertial coordinates of the CM and u, υ are the surge and sway velocities respectively defined in the body-fixed frame. The orientation of the vehicle is described by the angle ψ and r is its yaw velocity. The dynamic model used for the control design is that of an AUV since it is the most inclusive and encompasses the dynamics of the other two: assuming that the hydrodynamic drag terms of order higher than two are negligible, and the heave, pitch, and roll motions can be neglected, the dynamics for a neutrally buoyant torpedo shaped AUV, in horizontal motion, is expressed by the following equations [2]:

$$\dot{u}=\frac{m_{22}}{m_{11}}\upsilon r-\frac{d_{11}}{m_{11}}u-\frac{d_{u1}}{m_{11}}u|u|+\frac{1}{m_{11}}F_u \tag{2a}$$

$$\dot{\upsilon}=-\frac{m_{11}}{m_{22}}ur-\frac{d_{22}}{m_{22}}\upsilon-\frac{d_{\upsilon 1}}{m_{22}}\upsilon|\upsilon| \tag{2b}$$

$$\dot{r}=\frac{m_{11}-m_{22}}{m_{33}}u\upsilon-\frac{d_{33}}{m_{33}}r-\frac{d_{r1}}{m_{33}}r|r|+\frac{1}{m_{33}}F_r \tag{2c}$$

where the constants m_{11}, m_{22}, and m_{33} represent the combined inertia and added mass (negligible for the HC) terms, and the constants d_{11}, d_{u1}, d_{22}, $d_{\upsilon 1}$, d_{33}, and d_{r1} represent the hydrodynamic (aerodynamic for the HC) drag terms. The variable F_u denotes control force along the surge motion of the vehicle and F_r denotes control torque around the z axis of the body-fixed frame. There is no side thruster to control sway motion, so (2b) is uncontrolled and the MV constitutes an underactuated dynamical system. The aforementioned control configuration can be realized e.g. by providing the MV with two horizontal stern propellers or with a stern propeller and a rudder, Fig. 1.

3. Trajectory Planning

In this section, the main points regarding the reference trajectory planning methodology are stated. The only restriction on this trajectory is that it must be sufficiently "smooth", i.e., a continuous curve and three times differentiable with respect to time.

3.1 Path Kinematics

Let $x_R(t), y_R(t)$ be the time parameterized, inertial position of a point P on the planar path to be tracked by the MV's CM. The corresponding velocities and accelerations are $\dot{x}_R(t), \dot{y}_R(t), \ddot{x}_R(t), \ddot{y}_R(t)$. The subscript "R" indicates a reference variable. Omitting time dependence notation, the magnitude of the velocity vector $\mathbf{v}_p$, its direction β, and their derivatives are

$$v_p=\|\mathbf{v}_p\|=\sqrt{\dot{x}_R^2+\dot{y}_R^2} \tag{3}$$

$$\beta=\tan^{-1}\left(\dot{y}_R/\dot{x}_R\right) \tag{4}$$

$$\dot{v}_p=(\dot{x}_R\ddot{x}_R+\dot{y}_R\ddot{y}_R)\Big/(\sqrt{\dot{x}_R^2+\dot{y}_R^2}) \tag{5}$$

$$\omega=\dot{\beta}=(\dot{x}_R\ddot{y}_R-\dot{y}_R\ddot{x}_R)\Big/(\dot{x}_R^2+\dot{y}_R^2) \tag{6}$$

3.2 Vehicle's Dynamics on the Path

Considering the dynamics -with linear drag force for simplicity- of the MV as it tracks the reference path, let u_R, υ_R, r_R denote the body-fixed velocities of the vehicle. Thus, the magnitude of the velocity vector of the CM is

$$v_R=\|\mathbf{v}_R\|=\sqrt{u_R^2+\upsilon_R^2} \tag{7}$$

The reference orientation ψ_R i.e., the angle between the inertial X axis and the body x axis is the algebraic sum of the angle β and an angle γ, Fig. 2. The latter is created as a consequence of the dynamics of the vehicle as this rotates. Specifically, looking at (2b) and considering that the CM of the MV tracks the path, we see that because of surge and yaw motions, the coupling term $u_R r_R$ gives rise to a sway motion υ_R. A direct result is the appearance of γ which is expressed by

$$\gamma=\tan^{-1}(\upsilon_R/u_R) \tag{8}$$

Tracking, imposes two geometric constraints: Equality of v_p and v_R, and algebraic consistency of the angles, as depicted in Fig. 2:

$$v_p = v_R \Rightarrow \sqrt{\dot{x}_R^2 + \dot{y}_R^2} = \sqrt{u_R^2 + \upsilon_R^2} \tag{9}$$

$$\psi_R = \beta \pm \gamma = \tan^{-1}(\dot{y}_R / \dot{x}_R) \pm \tan^{-1}(\upsilon_R / u_R) \tag{10}$$

In (10), the sign "$\pm$" depends on the curvature of the trajectory. Also, $r_R = \dot{\psi}_R$. The algebraic system of the last derivative, (9), along with the dynamic constraint imposed by the unactuated dynamic equation (2b), may be solved for one of $\dot{\upsilon}_R$ or $\dot{u}_R$:

$$\begin{aligned}(m_{11} - m_{22})\dot{u}_R = (1/u_R v_p)(d_{22} u_R^2 v_p - d_{22} v_R^3 - \\ m_{11}\omega u_R v_p \sqrt{v_p^2 - u_R^2} + m_{11} u_R^2 \dot{v}_p - m_{22}\dot{v}_p v_p^2),\ u_R(t=0) \neq 0\end{aligned} \tag{11}$$

In case of an SV or an AUV, where $m_{11} \neq m_{22}$, (11) can be solved for $\dot{u}_R$ and integrated numerically to give u_R. In the case of an HC, where $m_{11} = m_{22}$, (11) reduces to an algebraic equation that can be solved for u_R. Note that (11), is obtained using a linear drag force; when quadratic drag is included, see (2b), we consider the sign of the additional drag term. Once u_R is computed the required open-loop control force and torque are obtained from (2a) and (2c), with the help of (9) and (10).

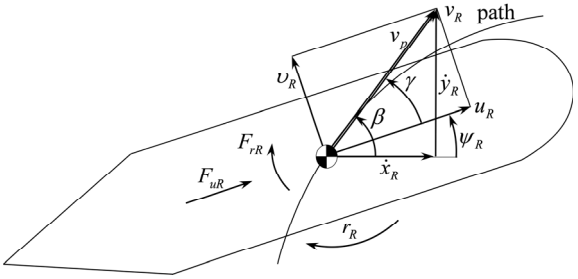

Fig. 2. An MV moving along a planar path.

As an illustration of the developed planning algorithm, consider the planar circular trajectory described by

$$x_R = 10\sin(0.01t) \tag{12a}$$

$$y_R = 10\cos(0.01t) \tag{12b}$$

in meters, along with their first and second derivatives. The MV system parameters in (2) are presented in Table I and taken from: [9] for HC, [13] for SV, and [8] for the AUV. Using (3) - (11) the body-fixed reference values and the angle γ, necessary for the three vehicles to track the circle, are computed and displayed in Table II. We observe that the angle γ corresponding to AUV is the largest. This is due to the quadratic drag in (2b) which causes larger centrifugal forces, trying to force the vehicle out of its path. To counteract these, the AUV must turn its body x axis even further towards the inside of the circle. Hence, when paths with nonzero curvature are to be tracked, the reference orientation ψ_R of the vehicle does not coincide with the angle between $\mathbf{v}_p$ and the X axis but depends on the trajectory and the MV dynamics (10).

Next, the computed reference values are used with the developed closed-loop trajectory-tracking controller.

TABLE I. Dynamic Models' Constants

Symbol (Units)	HC	SV	AUV
m_{11} (kg)	5.15	120×10^3	215
m_{22} (kg)	5.15	177.9×10^3	265
m_{33} $(kg\cdot m^2)$	0.047	636×10^5	80
d_{11} (kg/s)	4.5	215×10^2	70
d_{22} (kg/s)	4.5	147×10^3	100
d_{33} $(kg\cdot m^2/s)$	0.41	802×10^4	50
d_{u1} (kg/m)	0	0	100
$d_{\upsilon 1}$ (kg/m)	0	0	200
d_{r1} $(kg\cdot m^2)$	0	0	100

TABLE II. Reference Values

Symbol (Units)	HC	SV	AUV
u_R (m/s)	0.1	0.1	0.1
$\dot{u}_R$ (m/s^2)	0	0	0
υ_R (m/s)	0.011	0.0008	0.0021
$\dot{\upsilon}_R$ (m/s^2)	0	0	0
r_R (r/s)	–0.01	–0.01	–0.01
$\dot{r}_R$ (r/s^2)	0	0	0
γ (deg)	0.656	0.0082	1.23

4. Trajectory Tracking Control Design

In this section, the basic steps of the tracking controller design are highlighted. We assume bounded reference body-fixed velocities and nonzero surge velocity.

4.1 Error Dynamics Formulation

Using the states of the vehicle and the reference variables, the tracking errors are defined as $u_e = u - u_R$, $\upsilon_e = \upsilon - \upsilon_R$, $r_e = r - r_R$, $x_e = x - x_R$, $y_e = y - y_R$, $\psi_e = \psi - \psi_R$. Substituting for u, υ, r, x, y, and ψ in (1) and (2) we obtain the error dynamics as follows. From kinematics it is:

$$\dot{\mathbf{x}}_e = \mathbf{R}\mathbf{u}_e + \mathbf{R}_{\psi,\psi_R}\mathbf{u}_R \tag{13a}$$

$$\dot{\psi}_e = r_e \tag{13b}$$

where $\mathbf{x}_e \triangleq [x_e, y_e]^T$, $\mathbf{u}_e \triangleq [u_e, \upsilon_e]^T$, $\mathbf{u}_R \triangleq [u_R, \upsilon_R]^T$, and

$$\mathbf{R}(\psi) = \mathbf{R} \triangleq \begin{bmatrix} \cos\psi & -\sin\psi \\ \sin\psi & \cos\psi \end{bmatrix} \tag{14a}$$

$$\mathbf{R}_{\psi,\psi_R} \triangleq \mathbf{R}(\psi) - \mathbf{R}(\psi_R) \tag{14b}$$

Using the model of an MV with linear drag -for simplicity of presentation- we obtain

$$\dot{u}_e = \frac{m_{22}}{m_{11}}\left(\upsilon_e r_e + \upsilon_e r_R + \upsilon_R r_e\right) - \frac{d_{11}}{m_{11}}u_e + \frac{\left(F_u - F_{uR}\right)}{m_{11}} \tag{15a}$$

$$\dot{\upsilon}_e = -\frac{m_{11}}{m_{22}}\left(u_e r_e + u_e r_R + u_R r_e\right) - \frac{d_{22}}{m_{22}}\upsilon_e \tag{15b}$$

$$\dot{r}_e = \frac{m_{11}-m_{22}}{m_{33}}\left(u_e \upsilon_e + u_e \upsilon_R + u_R \upsilon_e\right) - \frac{d_{33}}{m_{33}} r_e + \frac{\left(F_r - F_{rR}\right)}{m_{33}} \tag{15c}$$

4.2 Error Dynamics Stabilization

The control objective now is to stabilize the error dynamics. Towards this, and taking

$$F_u = F_{uR} + d_{11}u_e - m_{22}(\upsilon_e r_e + \upsilon_e r_R + \upsilon_R r_e) + m_{11}\tau_u \tag{16}$$

$$F_r = F_{rR} + d_{33} r_e + (m_{22} - m_{11})(u_e \upsilon_e + u_e \upsilon_R + u_R \upsilon_e) + m_{33}\tau_r \tag{17}$$

yields a partial linearized system consisting of (13a,b), (15b), along with the integrators

$$\dot{u}_e = \tau_u \tag{18}$$

$$\dot{r}_e = \tau_r \tag{19}$$

where τ_u and τ_r are auxiliary controls along the surge and yaw motions respectively. F_{uR} and F_{rR} are given from reference dynamics obtained in Section 3. In the case of quadratic drag, its effects are compensated for in the actuated dynamics (15a,c) but not in (15b).

Next, backstepping, and nonlinear damping [16], and Young's inequality [6] are employed as our design tools.

Step 1. Considering the subsystem (13a), we take as virtual control the vector $\mathbf{u}_e = [u_e, \upsilon_e]^T$ and as a bounded disturbance (for bounded u_R and υ_R) the vector $\boldsymbol{\delta} \triangleq \mathbf{R}_{\psi,\psi_R}\mathbf{u}_R = [\delta_1, \delta_2]^T$. Choosing

$$V_1 = \mathbf{x}_e^T \mathbf{x}_e / 2 \tag{20}$$

the desired expressions for the virtual controls are

$$\mathbf{u}_{e,des} = -\mathbf{R}^T(\mathbf{K}+\mathbf{K}_1)\mathbf{x}_e \triangleq \boldsymbol{\alpha}(\mathbf{x}_e) = [\alpha_u, \alpha_\upsilon]^T \tag{21}$$

where $\mathbf{K} = diag(k,k)$ and $\mathbf{K}_1 = diag(k_1,k_1)$ are positive-definite gain matrices. Then,

$$\dot{V}_1 = -\mathbf{x}_e^T(\mathbf{K}+\mathbf{K}_1)\mathbf{x}_e + \mathbf{x}_e^T\boldsymbol{\delta} \le -\mathbf{x}_e^T\mathbf{K}\mathbf{x}_e + [(\delta_1^2+\delta_2^2)/4k_1] \tag{22}$$

Increasing k_1, $(\delta_1^2+\delta_2^2)/4k_1$ becomes arbitrarily small.

Step 2. Since $\mathbf{u}_e$ is not a true control, we have to introduce the error $\mathbf{z}_u = [z_u, z_\upsilon]^T = [u_e - \alpha_u, \upsilon_e - \alpha_\upsilon]^T$ in the controlled position equations as follows:

$$\dot{\mathbf{x}}_e = -(\mathbf{K}+\mathbf{K}_1)\mathbf{x}_e + \mathbf{R}\mathbf{z}_u + \boldsymbol{\delta} \tag{23a}$$

$$\dot{z}_u = \tau_u - \dot{\alpha}_u \tag{23b}$$

$$\dot{z}_\upsilon = -(m_{11}/m_{22})(u_e r_e + u_e r_R + u_R r_e) - (d_{22}/m_{22})\upsilon_e - \dot{\alpha}_\upsilon \tag{23c}$$

The task now is to stabilize the error variables z_u and z_υ. To stabilize z_u, we choose

$$V_2 = V_1 + z_u^2/2 \tag{24}$$

Its time derivative becomes

$$\dot{V}_2 = \mathbf{x}_e^T[-(\mathbf{K}+\mathbf{K}_1)\mathbf{x}_e + \mathbf{R}\mathbf{z}_u + \boldsymbol{\delta}] + z_u[\tau_u - \dot{\alpha}_u] \tag{25}$$

Using (22), and after some straightforward algebraic manipulations, (25) becomes

$$\begin{aligned}\dot{V}_2 \le & -\mathbf{x}_e^T\mathbf{K}\mathbf{x}_e + [(\delta_1^2+\delta_2^2)/4k_1] + x_e(z_u\cos\psi \\ & - z_\upsilon \sin\psi) + y_e(z_u\sin\psi + z_\upsilon\cos\psi) + \\ & z_u[\tau_u + (k+k_1)u_e + (k+k_1)(\delta_1\cos\psi + \delta_2\sin\psi)]\end{aligned} \tag{26}$$

Young's inequality for a positive k_2 gives

$$\begin{aligned}& x_e(z_u\cos\psi - z_\upsilon\sin\psi) + y_e(z_u\sin\psi + z_\upsilon\cos\psi) \\ & < k_2(x_e^2+y_e^2) + [(z_u^2+z_\upsilon^2)/4k_2]\end{aligned} \tag{27}$$

and (26) becomes

$$\begin{aligned}\dot{V}_2 \le & -(k-k_2)x_e^2 - (k-k_2)y_e^2 + [(\delta_1^2+\delta_2^2)/4k_1] \\ & + [(z_u^2+z_\upsilon^2)/4k_2] + z_u[\tau_u + (k+k_1)u_e + \\ & (k+k_1)(\delta_1\cos\psi + \delta_2\sin\psi)]\end{aligned} \tag{28}$$

Choosing $k > k_2$ the first two terms become nonpositive. The fourth term is discussed in the next steps. Setting

$$\tau_u = -(k+k_1)u_e - c_u z_u - k_u z_u (k+k_1)^2(\cos^2\psi + \sin^2\psi) \tag{29}$$

with k_u, $c_u > (1/4k_2)$ positive constants, (28) becomes

$$\begin{aligned}\dot{V}_2 \le & -(k-k_2)x_e^2 - (k-k_2)y_e^2 - c_u z_u^2 + \\ & [(1/4k_1)+(1/4k_u)](\delta_1^2+\delta_2^2) + [(z_u^2+z_\upsilon^2)/4k_2] \\ = & -(k-k_2)x_e^2 - (k-k_2)y_e^2 - [c_u - (1/4k_2)]z_u^2 + \\ & [(1/4k_1)+(1/4k_u)](\delta_1^2+\delta_2^2) + [(z_\upsilon^2)/4k_2]\end{aligned} \tag{30}$$

Step 3. Next, we stabilize the subsystem consisting of (13b), and (23c) which is rewritten as

$$\dot{z}_\upsilon = -(m_{11}/m_{22})ur_e + \delta_\upsilon \tag{31}$$

where

$$\begin{aligned}\delta_\upsilon = & -(m_{11}/m_{22})u_e r_R + [k + k_1 - (d_{22}/m_{22})]\upsilon_e \\ & + (k+k_1)(\delta_2\cos\psi - \delta_1\sin\psi)\end{aligned} \tag{32}$$

The above term is bounded provided that u_e and υ_e are bounded. This is achieved once the complete system controller is designed at the final step. Considering the error $r_e = \alpha_r$ as virtual control, assuming $u \neq 0$, choosing

$$V_3 = V_2 + \left(z_\upsilon^2 + \psi_e^2\right)/2 \tag{33}$$

and taking into account (30), we obtain

$$\dot{V}_3 \le W + b - z_\upsilon[(m_{11}/m_{22})u\alpha_r - \delta_\upsilon] + \psi_e\alpha_r + [(z_\upsilon^2)/4k_2] \tag{34}$$

where

$$W = -(k-k_2)x_e^2 - (k-k_2)y_e^2 - [c_u - (1/4k_2)]z_u^2 \tag{34'}$$

$$b = [(1/4k_1)+(1/4k_u)](\delta_1^2+\delta_2^2) \tag{34"}$$

Setting,

$$\alpha_r = -c_r[-(m_{11}/m_{22})uz_\upsilon + \psi_e] \tag{35}$$

for some c_r positive, (34) becomes

$$\begin{aligned}\dot{V}_3 \le & W + b - c_r(m_{11}uz_\upsilon/m_{22})^2 - c_r\psi_e^2 + z_\upsilon\delta_\upsilon \\ & + 2c_r(m_{11}/m_{22})uz_\upsilon\psi_e + (z_\upsilon^2/4k_2)\end{aligned} \tag{36}$$

For some positive k_z and k_ψ, the uncertain terms can be transformed in order for (36) to become

$$\dot{V}_3 \le W + b - c_r \psi_e^2 + (\delta_\upsilon^2 / 4k_z) - [c_r (m_{11}u / m_{22})^2 - (k_z + k_\psi + (1/4k_2))] z_\upsilon^2 + (c_r^2 / k_\psi)(m_{11} u \psi_e / m_{22})^2 \quad (37)$$

Step 4. Introducing the error $z_r = r_e - \alpha_r$ we have:

$$\dot{z}_\upsilon = -(m_{11}u / m_{22})(\alpha_r + z_r) + \delta_\upsilon \quad (38a)$$

$$\dot{\psi}_e = \alpha_r + z_r \quad (38b)$$

$$\dot{z}_r = \tau_r - \dot{\alpha}_r \quad (38c)$$

Using (37) and choosing

$$V_4 = V_3 + z_r^2 / 2 \quad (39)$$

we have

$$\dot{V}_4 \le W + b - c_r \psi_e^2 + (\delta_\upsilon^2 / 4k_z) - [c_r (m_{11}u / m_{22})^2 - (k_z + k_\psi + (1/4k_2))] z_\upsilon^2 + (c_r^2 / k_\psi)(m_{11} u \psi_e / m_{22})^2 + z_r [\tau_r + z_\upsilon + \psi_e + c_r [(m_{11}u / m_{22})^2 + 1] r_e - c_r (m_{11}u / m_{22}) \delta_\upsilon] \quad (40)$$

With positive c and k_c, and taking

$$\tau_r = -z_\upsilon - \psi_e - c_r [(m_{11}u / m_{22})^2 + 1] r_e - [c + k_c (c_r m_{11} u / m_{22})^2] z_r \quad (41)$$

and after some manipulations, (40) becomes

$$\dot{V}_4 \le W + b - [c_r - ((c_r m_{11} u)^2 / m_{22}^2 k_\psi)] \psi_e^2 - [c_r (m_{11}u / m_{22})^2 - (k_z + k_\psi + k_3 ((m_{11}u / m_{22})^2 + 1) + (1/4k_2))] z_\upsilon^2 - [c - (1/4k_3)] z_r^2 - k_c [z_r c_r (m_{11}u / m_{22}) + (\delta_\upsilon / 2k_c)]^2 + [(1/4k_z) + (1/4k_c)] \delta_\upsilon^2 \quad (42)$$

The third and fourth terms must be negative definite. The compatibility of these inequalities gives the range of the values of c_r. The term $[(1/4k_z) + (1/4k_c)]\delta_\upsilon^2$ is bounded and can be made arbitrarily small increasing the gains k_z or k_c. Also it must be $c > (1/4k_3)$. Setting

$$\Delta = b + [(1/4k_z) + (1/4k_c)]\delta_\upsilon^2 \quad (43)$$

we can conclude that there is a positive constant ξ, sufficiently small, such that

$$\dot{V}_4 \le -\xi V_4 + \Delta \quad (44)$$

Utilizing the Comparison Lemma [6], we conclude that

$$V_4 \le e^{-\xi t} V_4(0) + (\Delta / \xi) \quad (45)$$

which means that the tracking errors remain in a bounded set around zero. At this result we arrived using the controls in (16), and (17), along with (29) and (41).

5. Simulation Results

The tracking performance of the designed controller was tested using the dynamic models of the three MVs in computer simulations. They showed quick convergence of the tracking errors to zero, smooth transient response, low control effort, and robustness, even in the case of large initial errors. To illustrate the performance of the proposed trajectory planning and tracking control methods, typical simulation results are presented.

The desired circular trajectory (12) and the corresponding reference body-fixed velocities and orientation, Table II, are used here again. The dynamic models of the three MVs are the ones presented in (2) with the parameters in Table I. The results were obtained with the following controller gains: for the HC $k = c_u = 0.3$, $k_1 = k_u = 0.5$, $c_r = 0.1$, $c = k_c = 0.4$; for the SV $k = c_r = 0.5$, $k_1 = k_u = c_u = c = k_c = 0.7$; for the AUV $k = 1$, $k_1 = k_u = k_c = 3$, $c_u = c_r = c = 2$. The larger values for the AUV gains are justified by the fact that the quadratic drag force increases the term δ_υ in (30) which directly affects the errors and this must be compensated for by a higher control effort.

The three vehicles start with zero initial velocities. The initial position and orientation errors are $|x_e| = 0.5\,m$, $|y_e| = 1\,m$, and $|\psi_e| = 15^\circ$ for all three vehicles. In Fig. 3, the required controls and the tracking errors of the HC are depicted. After a short time period of transition, the errors converge smoothly to a set of zero, of the order of $10^{-5}\,m/s$ or rad/s for velocities, and $10^{-5}\,m$ or deg for pose, and slowly oscillate within. In Fig. 4, the response of the SV to the circular trajectory is shown. Again, after a smooth transition period the errors converge and remain to a very small set of zero verifying the theoretical results. In Fig. 5, we observe the same smooth transient response for the AUV. However, the time needed for the tracking errors to converge is longer. Also, the tracking errors are of the order of $10^{-3}\,m/s$ or rad/s for velocities, and $10^{-2}\,m$ or deg for pose.

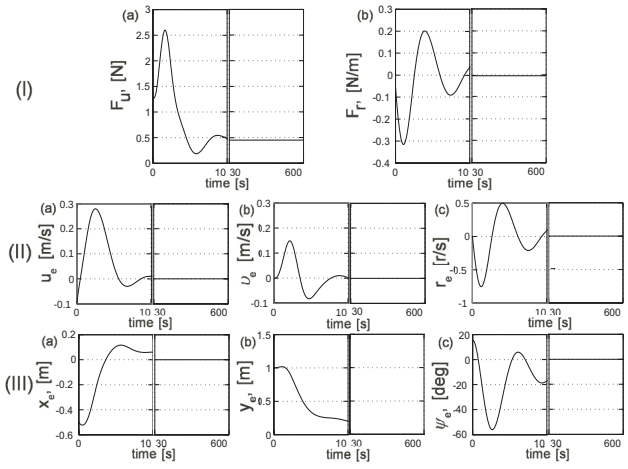

Fig. 3. HC response. I (a, b) control force & control torque. II (a, b, c) linear and angular velocity tracking errors. III (a, b, c) Position and angular tracking errors.

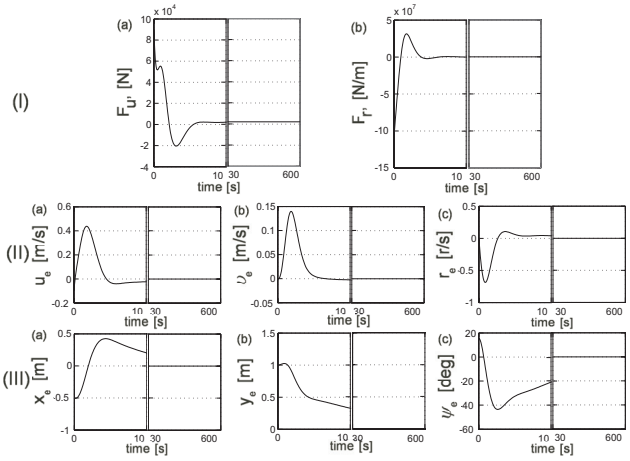

Fig. 4. SV response. I (a, b) control force & control torque. II (a, b, c) linear and angular velocity tracking errors. III (a, b, c) Position and angular tracking errors.

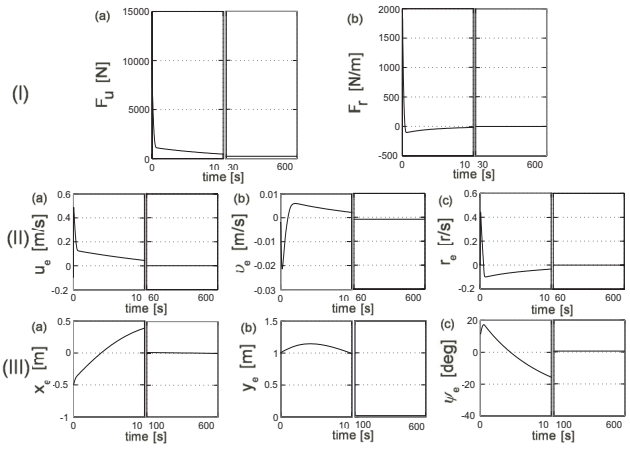

Fig. 5. AUV response. I (a, b) control force & control torque. II (a, b, c) linear and angular velocity tracking errors. III (a, b, c) Position and angular tracking errors.

6. Conclusions

In this paper, we addressed the combined problem of trajectory planning and tracking control for underactuated MVs with different dynamic models in planar motion. The reference trajectory, consisting of the desired inertial position and corresponding velocities, was designed to be a feasible "state-space" trajectory i.e. consistent with each of the three vehicle dynamics. Based on the dynamics and the reference velocities, the reference orientation is also computed. Using the reference and vehicle states, the system dynamics was transformed to the error dynamics. Design methods such as partial state-feedback linearization, backstepping and nonlinear damping were used to drive the tracking error to a small neighborhood of the origin that can be reduced arbitrarily. Computer simulations illustrated the developed trajectory planning and tracking control scheme.

7. Acknowledgements

Support by the NTUA Senator Committee of Basic Research Programme "Protagoras", R.C. No. 10, is acknowledged.

References:

[1] Yuh, J., "Design and Control of Autonomous Underwater Robots: A Survey", *Int. J. Control,* No 8, 2000, pp. 7-24.

[2] Fossen, T. I., *Guidance and Control of Ocean Vehicles,* New York: Wiley, 1994.

[3] Papadopoulos, E., Poulakakis, I., and Papadimitriou, I., "On Path Planning and Obstacle Avoidance for Nonholonomic Mobile Manipulators: A Polynomial Approach", *Int. Journal of Robotics, Research,* V. 21(4), 2002, pp. 367-383.

[4] Dubowsky, S., and Papadopoulos, E., "The Kinematics, Dynamics and Control of Free-flying and Free-floating Space Robotic Systems", *IEEE Tran. Rob. Autom.,* Vol. 9, No 5, October 1993, pp. 531-543.

[5] Kaminer, I., Pascoal, A., Hallberg, E., and Silvestre, C., "Trajectory Tracking for Autonomous Vehicles: An Integrated Approach to Guidance and Control", *J. Guid., Con. Dyn.,* V. 21 (1), Jan.–Feb. 1998, pp. 29-38.

[6] Khalil, H. K., *Nonlinear Systems,* 2nd ed, Prentice Hall, Upper Saddle River, 1996.

[7] Reyhanoglou, M., "Exponential Stabilization of an Underactuated Autonomous Surface Vessel", *Automatica,* 33(12), 1997, pp. 2249-2254.

[8] Pettersen, K. Y., and Egeland, O., "Time-Varying Exponential Stabilization of the Position and Attitude of an Underactuated Autonomous Underwater Vehicle", *IEEE Tran. Aut. Con.,* V. 44(1), Jan. 1999, pp. 112-115.

[9] Aguiar, P. A., Cremean, L., and Hespanha, J. P., "Position Tracking for a nonlinear Underactuated Hovercraft: Controller Design and Experimental Results", *Proc. IEEE CDC,* Dec. 2003.

[10] Aguiar, P. A., and Hespanha, J. P., "Position Tracking of Underactuated Vehicles", *ACC,* June 2003.

[11] Lefeber, E., Pettersen, K. Y., and Nijmeijer, H., "Tracking Control of an Underactuated Ship", *IEEE Tran. Con. Sys. Tec.,* 11(1), January 2003, pp. 52-61.

[12] Jiang, Z. P., "Global Tracking Control of Underactuated Ships by Lyapunov's Direct Method", *Automatica,* 38(1), 2002, pp. 301-309.

[13] Do, K., D., Jiang, Z. P., and Pan, J., "Robust Adaptive Path Following of Underactuated Ships", *Automatica,* V. 40, 2004, pp. 929-944.

[14] Behal, A., Dawson, D. M., Dixon, W. E., and Fang, Y., "Tracking and Regulation Control of an Underactuated Surface Vessel with Nonintegrable Dynamics", *IEEE Tran. Aut. Con.,* V. 47(3), Mar. 2002, pp. 495-500.

[15] Repoulias, F., and Papadopoulos, E., "Trajectory Planning and Tracking Control Design of Underactuated AUVs", *Proc. IEEE Int. Con. on Rob. .Aut.*, Barcelona, Spain, April 2005,pp.1622-1627.

[16] Krstic, M., Kanellakopoulos, I., and Kokotovic, P., *Nonlinear and Adaptive Control Design,* New York: Wiley, 1995.